Parametric Modeling and Hydrodynamic Analysis of Underwater High Performance Propeller

Jixin Liu[1, a], Tianhong Yan[1, b, *], Bo He[2, c], Hongbin Shen[1, d] and Jinliang Song[1, e]
[1]*Department of Mechanical and Electrical Engineering, China Jiliang University, Hangzhou 310018, China.*
[2]*Department of Information Science and Engineering, Ocean University of China, Qingdao 266100, China.*

Keywords: Openprop, AUV, Propeller, Three-dimensional Modeling, Hydrodynamic Analysis, Thrust Test.

Abstract: At present, the propeller-dependent drive system is still the mainstream propulsion mode of underwater vehicle. The propeller plays an important role in the whole propulsion system, and its effect directly affects the thrust, speed, efficiency and endurance of the underwater vehicle. The propeller used by autonomous underwater vehicle (AUV) should not only satisfy the demands of thrust and torque, but also high efficiency. In this paper, four kinds of airfoil propellers with different sizes and shapes are designed based on OpenProp software, and their performances are tested by thrust test. The comparison between the four kinds of airfoil propeller and the contrast between the airfoil propeller and the MAU type four-bladed propeller are made. In addition, a series of conclusions are drawn, which lays the foundation for designing the propeller with high efficiency and thrust.

1 INTRODUCTION

Overview of underwater navigation equipment, both large and small ships, yachts, lifeboats and various underwater vehicles such as warships, submarines are using propeller. Propeller propulsion is still one of the most important way of propulsion. Although it is not very efficient, but simple in structure and easy to apply. With the progress of manufacturing industry in China and the development of large-scale machine tools and numerical control technology, machining a propeller becomes more convenient. The design parameters and machining accuracy of propeller have a direct influence on the performance of propeller, which in turn affects the movement of underwater vehicle. Now the propeller machining process is very simple. When the three-dimensional software modeling is completed, model is imported into the CNC machine tool. After simple programming and tool setting, the machine tool automatically completes the processing, and the general accuracy can be guaranteed. Therefore, the design parameters are really affecting the performance of the propeller. The main parameters includes paddle type, blade shape and quantity, diameter, pitch ratio, disk ratio, longitudinal inclination, propeller convolute and the diameter of the rotor hub. When the propeller rotates, the side of the cut water is the leading edge, and the other side is the trailing edge. The surface of the blade pushing the water is called the leaf surface, the other side is called the leaf back. The leaf near the hub is the blade root, and the outer side is the blade tip (X. F. Xue, T. H. Yan, B. He, 2016). When the vehicle travels forward, the propeller turns clockwise look from the tail is right-rotor reverse propeller. When it rotates counterclockwise, it is the left-rotor positive propeller.

At present, the performance test method of the propeller is mainly three-dimensional model open water performance calculation (Z. Q. Yao, H. Gao, C. L. Yang, 2008; L. Huang, L. Chen, 2014; W. G. He, 2014; Y. W. Ding, J. M. Wu, Z. Q. Ma, 2018; X. M. Wang, S. Feng, 2018; X. S. Xie, Z. F. Jiang, L. Y. Qiu, 2015; J. M. Wu, Y. F. Lai, J. W. Li, 2016; F. D. Gao, C. Y. Pan, 2011; C. Y. Liu, K. Luo, Q. Guo, 2017; T. Zhang, C. J. Yang, B. W. Song, 2011). The advantages are low cost, save time and simple, but

Liu, J., Yan, T., He, B., Shen, H. and Song, J.
Parametric Modeling and Hydrodynamic Analysis of Underwater High Performance Propeller.
DOI: 10.5220/0008480601440154
In *Proceedings of 5th International Conference on Vehicle, Mechanical and Electrical Engineering (ICVMEE 2019)*, pages 144-154
ISBN: 978-989-758-412-1

the simulation results may not be accurate. Based on OpenProp and SolidWorks, four kinds right-rotor propellers used for AUV are designed. They are processed into physicals to verify the design parameters and propeller performance through thrust test. The airfoil propeller and the map propeller are compared, analyzed and summarized. Thrust test both have advantage and disadvantage. The advantage is that the result is accurate and reliable, and the disadvantage is high cost and spend long time.

2 THREE DIMENSIONAL MODELING OF PROPELLER

The four propellers tested in this paper are suitable for AUV. The AUV outer diameter is 324mm, total length is 3800mm approximately and the mass is 270kg in air. It is analyzed from the OpenProp parameter research module that the big diameter of the blade could improve the thrust and efficiency,

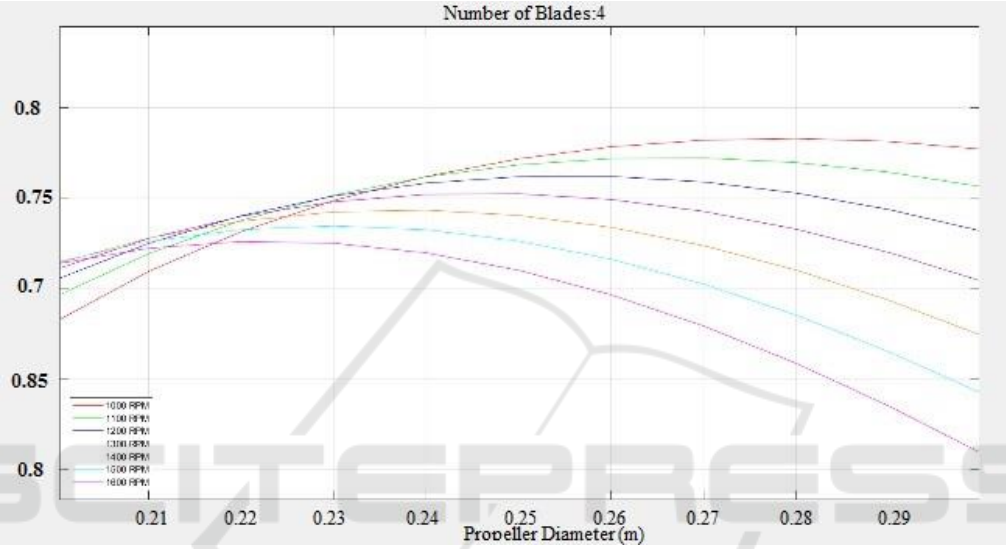

Figure 1. Parameter study curve.

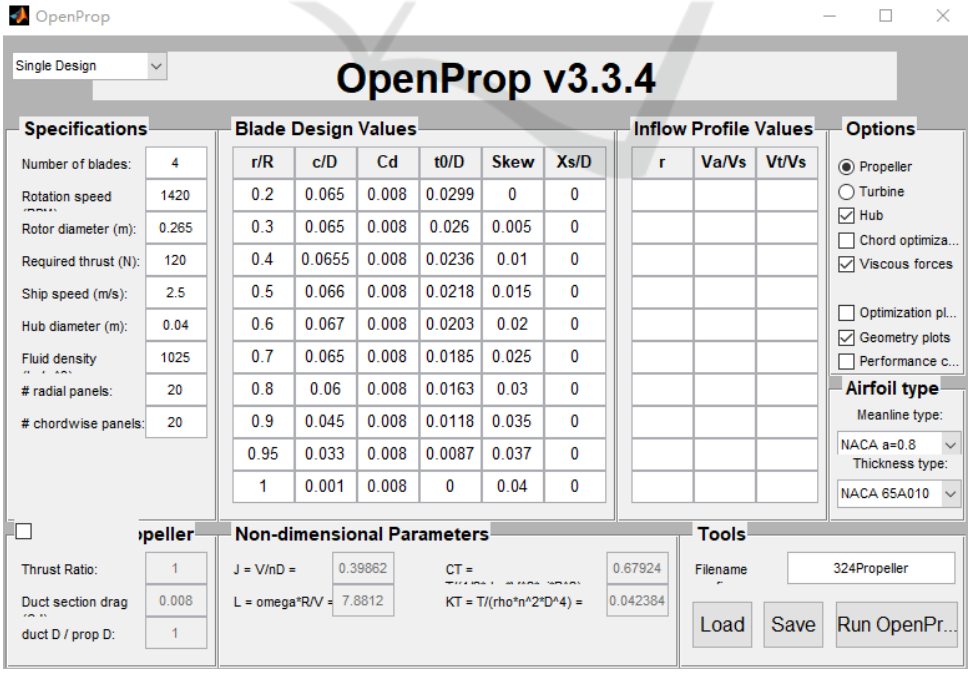

Figure 2. Single design module parameters.

but it can't exceed 85% of the outer diameter of the AUV (R. S. Duelley, 2011). From the parameter study curve as shown in Fig.1, the blade thickness type is NACA 65A010 and the diameter is 210mm, 245mm, 265mm. There are three-bladed propeller and four-bladed propeller. The rotation of them is right-rotor, and the propeller hub diameter is 30mm or 40mm.

The silver narrow four-bladed propeller with a diameter of 265 mm is taken as an example, and the rest will not be described in this paper. First of all, input the predetermined parameters in the single design module of OpenProp as shown in Fig.2, and run the program to generate the blade coordinate points. Secondly, organize the data in three-dimensional coordinate format to fulfill software's requirements, import the data into SolidWorks to generate the blade, and design the hub through the surface lofting and circumferential array (B. An, H. H. Zhu, S. D. Fan, 2017; Y. F. Qin, X. J. Sun, X. H. Lin, 2017). Then, add fillets at the root to increase the intensity and generate the final three-dimensional model as shown in Fig.3 to Fig.6.

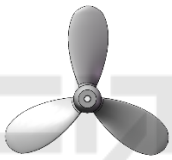

Figure 3. Silver wide three -bladed propeller.

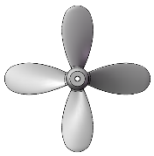

Figure 4. Silver wide four-bladed propeller.

Figure 5. Silver narrow three-bladed propeller.

Figure 6. Silver narrow four-bladed propeller.

3 THRUST TEST OF PROPELLER

The experiment platform of this test is a thrust test device as shown in Fig.7 and Fig.8. It is fixed on the pool filled with seawater. The lever principle and the equidistant force arm are used, and the lower arm is connected to the AUV ankle propulsion system. The upper arm is connected to the dynamometer. When the propeller rotates to generate the thrust, the AUV stern moves forward to drive the upper side to move backwards. The thrust is transmitted 1:1 to the dynamometer, and the thrust data can be read from the dynamometer.

The thrust test is carried out in order from low speed to high speed. The motor speed is changed from 500 to 5000 rpm, for every 500 rpm increase. The motor-to-propeller reduction ratio is 3.5. The rated voltage of the motor to drive propeller is 48V, and the peak current is set to 20A. Due to the low manufacturing precision of the thrust test device and the error of the underwater adjustment balance, the data displayed by the tension meter has a jump when the motor speed is below 1000 rpm. So the two pieces of data recorded at the beginning have no reference value. The test data is shown in Table 1 and Table 2. The black is a MAU type four-bladed propeller with a diameter of 180 mm. The silver wide four-bladed airfoil propeller has a diameter of 210 mm. The silver wide three-bladed airfoil propeller also has a diameter of 210 mm. The silver narrow four-bladed airfoil propeller diameter is 265mm, and the silver narrow three-bladed airfoil propeller diameter is 245mm.

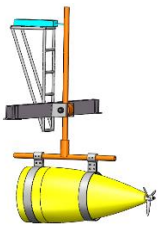

Figure 7. Three-dimensional drawing of thrust test device.

Figure 8. Physical drawing of thrust test device.

Table 1. Date of propeller thrust test one.

Motor Rotating Speed (n)	Silver Wide Four-bladed Propeller (Reverse)		Silver Wide Three-bladed Propeller (Reverse)		Silver Narrow Four-bladed Propeller (Reverse)		Silver Narrow Three-bladed Propeller (Reverse)	
	Current (A)	Thrust (N)	Current (A)	Thrust (N)	Current (A)	Thrust (N)	Current (A)	Thrust (N)
500	1.2	16.5	0.7	10.2	0.95	7	1.1	21.1
1000	4	38.2	2.1	22	2.9	29.8	4.1	56.3
1500	9.5	86	4.8	46	5.9	65.2	8.2	104
2000	14.7	115	8.5	89	11.8	128	14	179
2500	—	—	12.5	120	13	148	—	—
3000	—	—	—	—	—	—	—	—

Table 2. Date of propeller thrust test two.

Motor Rotating Speed (n)	Black Four-bladed Propeller (Correct)		Silver Wide Four-bladed Propeller (Correct)		Silver Wide Three-bladed Propeller (Correct)		Silver Narrow Four-bladed Propeller (Correct)		Silver Narrow Three-bladed Propeller (Correct)	
	Current (A)	Thrust (N)	Current (A)	Thrust (N)	Current (A)	Thrust (N)	Current (A)	Thrust (N)	Current (A)	Thrust (N)
500	0.3	20	0.3	15	0.15	12	0.3	16	0.25	17
1000	0.65	22	1	17	0.35	14	0.55	18	0.85	19
1500	1.3	25	2.1	20	0.9	15	2	19	1.8	22
2000	2.65	28	4.1	25	1.7	16	3.3	20	3.3	25
2500	4	40	6	35	3.1	22	5.1	25	5.1	26
3000	5.7	55	9	55	4	28	6.5	32	8	44
3500	8.7	78	13	78	6.5	45	8.7	43	11	60
4000	10	93	20	100	8.5	60	11.5	55	13.5	74
4500	13.5	125	—	—	12	90	17.5	70	20	100
5000	18	145	—	—	14.5	95	19	80	—	—

In reference (J. M. Wu, L. Zhong, E. W. Zhang, 2017), the propeller thrust characteristics of the underwater robot in reverse motion are studied. The test shows that the propeller can generate a large thrust at a lower speed after the reverse installation. And the current is much smaller than the current when the propeller is correct installation. However, after the reverse installation, the phenomenon of cavitation appeared. The phenomenon of cavitation of the wide blade is more obvious than that of the narrow blade. The influence of the cavitation factor on the hydrodynamic characteristics of the propeller blade is not only happened on the suction surface, but also the pressure surface. There is a non-negligible influence in reference (J. M. Wu, E. W. Zhang, L. Zhong, 2018). According to the relationship between the rotational speed and the vacuole summarized in the reference (J. M. Wu, E. W. Zhang, L. Zhong, 2018), further analysis and improvement are needed to make the cavitation phenomenon appear at high rotational speed, avoiding the occurrence at low rotational speed.

4 DATA ANALYSIS AND IMPROVEMENT

It can be clearly seen from Table 1 and Table 2 that the performance of the four airfoil propellers is not as good as the MAU type propeller tested in this paper when in the correct installation, and the performance in the reverse installation far exceeds the MAU type propeller. Further, the efficiency of each propeller is calculated from the data of the two tables and the equations (1) to (3).

$$P_1 = UI \tag{1}$$

$$P_2 = FV = F \times P \times D \times N/60 \tag{2}$$

$$\eta = P_2/P_1 \tag{3}$$

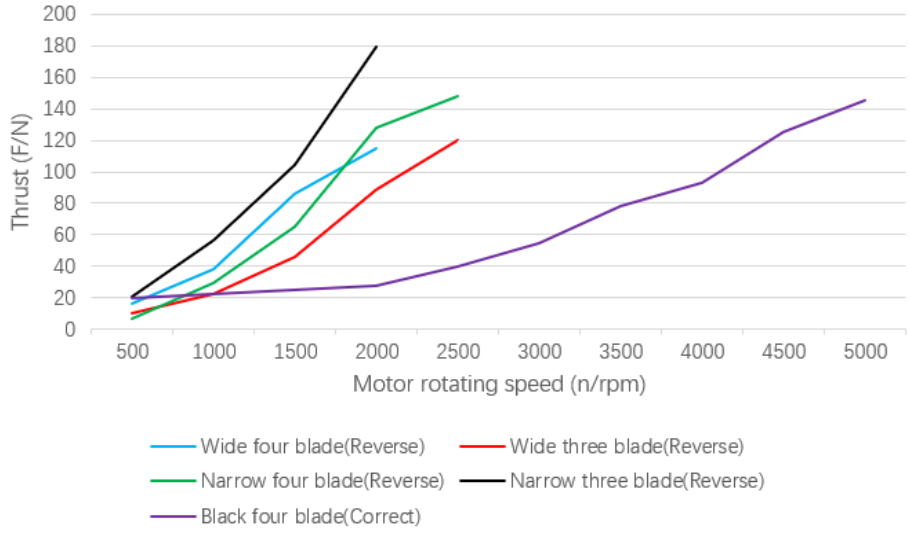

Figure 9. Relation curve between rotating speed and thrust.

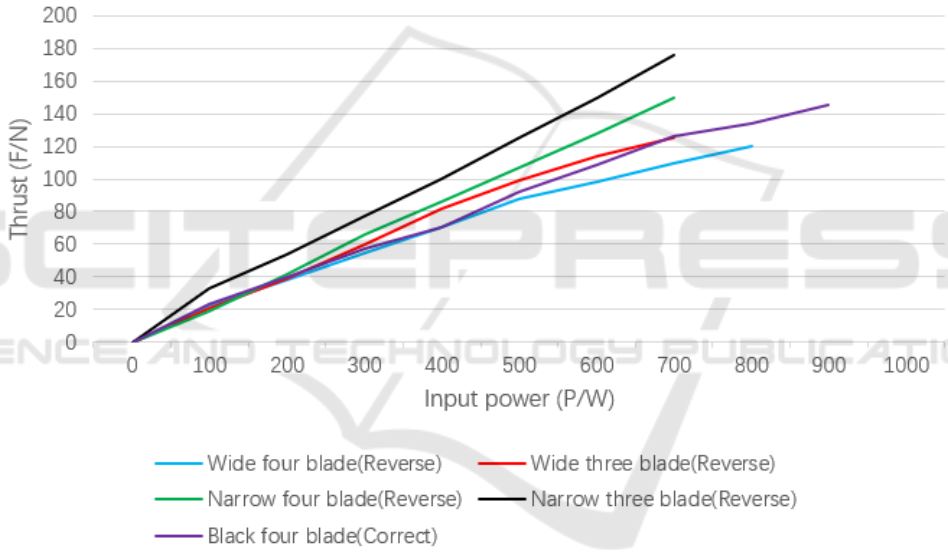

Figure 10. Relation curve between input power and thrust.

In the formula, P1 is the input power. U is the rated voltage of 48V. I is the current. P2 is the output power. F is the thrust. P is the pitch ratio. D is the propeller diameter. N is the propeller rotating speed, the speed after deceleration of motor speed. η is the efficiency of the propeller. When the propeller is correct installation and motor speed at 4000 rpm, the efficiency of the MAU type propeller is about 53%, and the efficiency of the four airfoil propellers is between 40% and 46%. When the propeller reverse installation and motor speed is 2000 rpm, the efficiency of the silver narrow three-bladed propeller and the silver narrow four-bladed propeller can reach about 60%.

As shown in Fig.9 and Fig.10, the silver narrow three-bladed propeller has the best performance when it is reversed installation, and secondly the silver narrow four-bladed propeller reversed installation. In reference (R. S. Duelley, 2011), three sets of chord/diameter parameters were studied based on the lift line theory, and the efficiency values of each group were compared as shown in Table 3. Considering the performance, efficiency, strength and ease of processing of the propeller, the final design parameters are given in reference (R. S. Duelley, 2011), as shown in Table 4.

Table 3. Three sets of chord/diameter parameters.

r/R	C_1/D_1	C_2/D_2	C_3/D_3
0.2	0.0800	0.0650	0.0530
0.3	0.0770	0.0770	0.0620
0.4	0.0730	0.0730	0.0650
0.5	0.0718	0.0718	0.0660
0.6	0.0680	0.0680	0.0670
0.7	0.0600	0.0600	0.0610
0.8	0.0500	0.0500	0.0500
0.9	0.0320	0.0320	0.0310
0.95	0.0200	0.0200	0.0200
1	0.0010	0.0010	0.0010
Efficiency	78.73%	78.74%	78.83%

Table 4. Final propeller geometry inputs.

r/R	t0/C	C/D	t0/D	Rake
0.2	0.4606	0.0650	0.0299	0
0.3	0.4001	0.0650	0.0260	0.005
0.4	0.3601	0.0655	0.0236	0.010
0.5	0.3302	0.0660	0.0218	0.015
0.6	0.3034	0.0670	0.0203	0.020
0.7	0.2841	0.0650	0.0185	0.025
0.8	0.2719	0.0600	0.0163	0.030
0.9	0.2632	0.0450	0.0118	0.035
0.95	0.2624	0.0330	0.0087	0.037
1	0.0000	0.0010	0.0000	0.040

According to the parameters of Table 4, the narrow four-bladed propeller shown in Fig.6 was designed. Through the thrust test and the actual application test, although the ideal thrust was generated, the autonomous underwater vehicle could not achieve at a high speed under high efficiency. The ratio of the chord/diameter of the above-mentioned silver narrow three-bladed propeller is about 1.7 times that of the narrow four-bladed propeller. The optimized design of the silver narrow three-bladed propeller is reduced to 210 mm in diameter. The chord/diameter ratio is kept 1.7 times. The thickness/diameter ratio is consistent with the narrow four-blade, enabling it to achieve high rotational speed while avoiding cavitation.

The optimized propeller is meshed by ICEM CFD and imported into Fluent for hydrodynamic performance simulation calculation (R. Muscari, G. Dubbioso, M. Viviani, A. D. Mascio, 2017; W. H. Lam, D. J. Robinso, G. A. Hamill, H. T. Johnston, 2012). The RNG k-epsilon turbulence model is selected because this model is suitable for calculating the rotational flow. Use MRF (A. Bhattacharyya, V. Krasilnikov, S. Steen, 2016; S. Sezen, A. Dogrul, C. Delen, S. Bal, 2018; M. M. Helal, T. M. Ahmed, A. A. Banawan, M. A. Kotb, 2018) to calculate the flow problem of the rotating domain. There are two domains, the flow domain called Fluid and the rotating domain called Rotating, and use the Interface to connect flow domain and rotating domain. The simulation calculation is set as the speed inlet, the pressure outlet. The inflow velocity is 2.5 m/s. The propeller rotating speed is 1400 rpm. The simulation calculation (X. F. Xue, T. H. Yan, B. He, 2016) is based on equations (4) to (7):

$$\frac{\partial}{\partial t}(\rho u_i) + \frac{\partial}{\partial x_j}(\rho u_i u_j) = -\frac{\partial p}{\partial x_i} + \frac{\partial \tau_{ij}}{\partial x_j} + \rho g_i + F_i \quad (4)$$

$$\tau_{ij} = \left[\mu\left(\frac{\partial u_i}{\partial x_j} + \frac{\partial u_j}{\partial x_i}\right)\right] - \frac{2}{3}\mu\frac{\partial u_l}{\partial x_l}\delta_{ij} \quad (5)$$

$$\rho\frac{\partial k}{\partial t} = \frac{\partial}{\partial x_i}\left[\left(\mu + \frac{\mu_t}{\sigma_k}\right)\frac{\partial k}{\partial x_i}\right] + G_k + G_b - \rho\varepsilon - Y_M \quad (6)$$

$$\rho\frac{\partial \varepsilon}{\partial t} = \frac{\partial}{\partial x_i}\left[\left(\mu + \frac{\mu_t}{\sigma_k}\right)\frac{\partial \varepsilon}{\partial x_i}\right] + C_{1\varepsilon}\frac{\varepsilon}{k}(G_k + G_{3\varepsilon}G_b) - C_{2\varepsilon}\rho\frac{\varepsilon^2}{k} \quad (7)$$

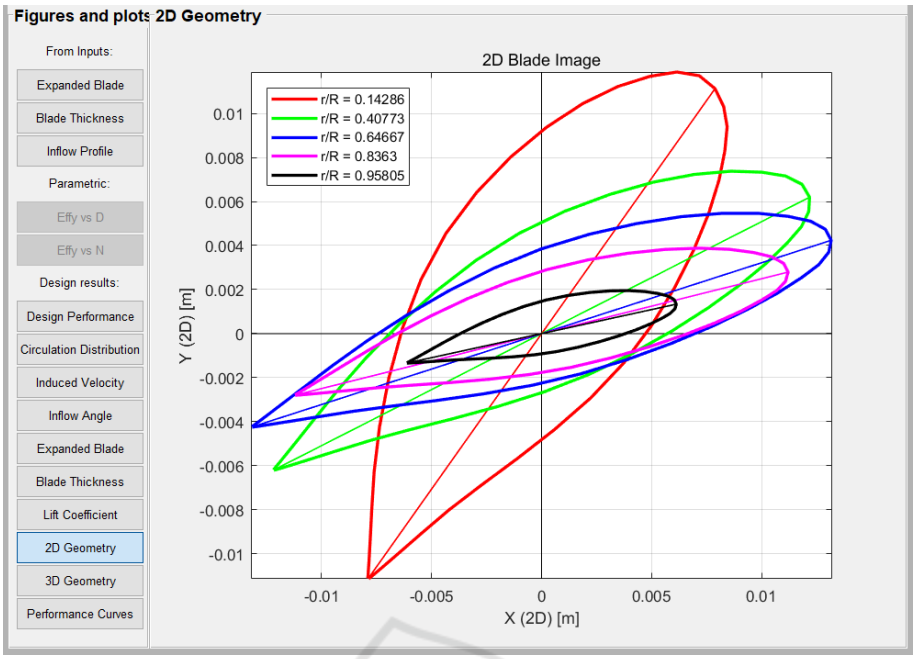

Figure 11. Optimized blade profile

Figure 12. Optimized narrow three-bladed propeller.

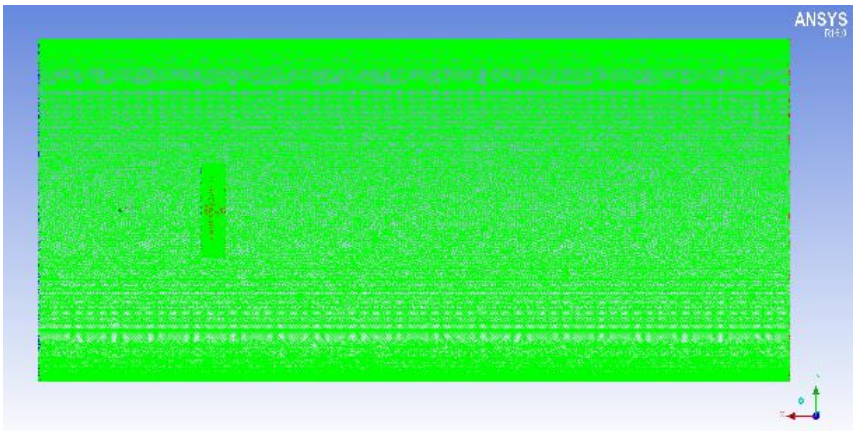

Figure 13. Mesh division of fluid and rotating domain.

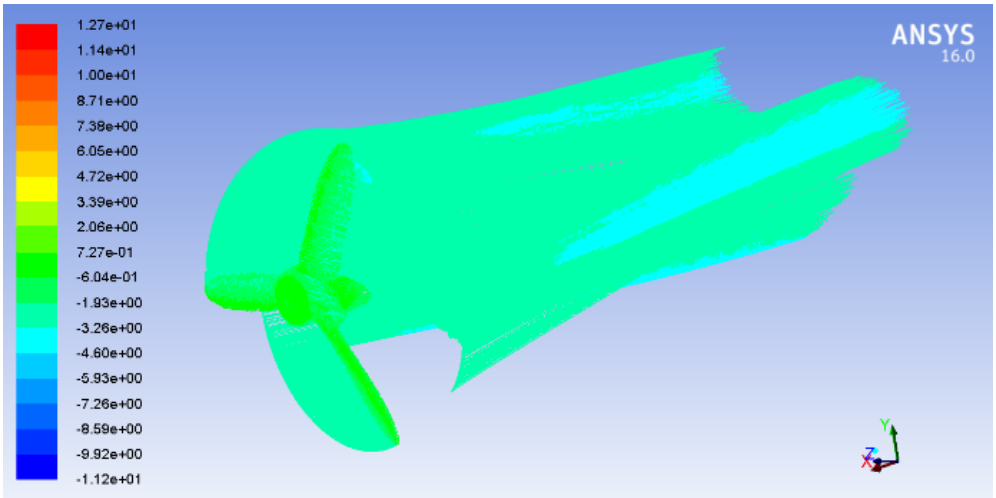

Figure 14. Axial velocity streamline diagram.

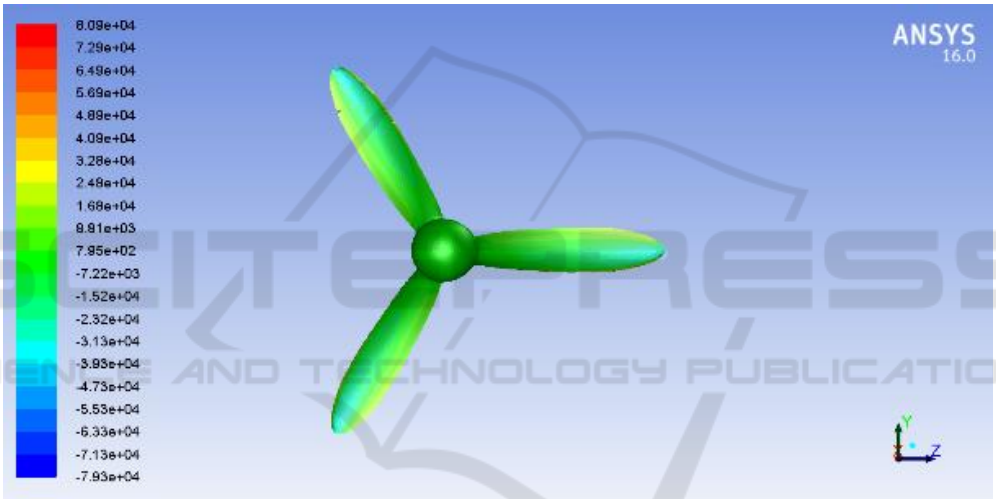

Figure 15. Propeller leaf pressure cloud map.

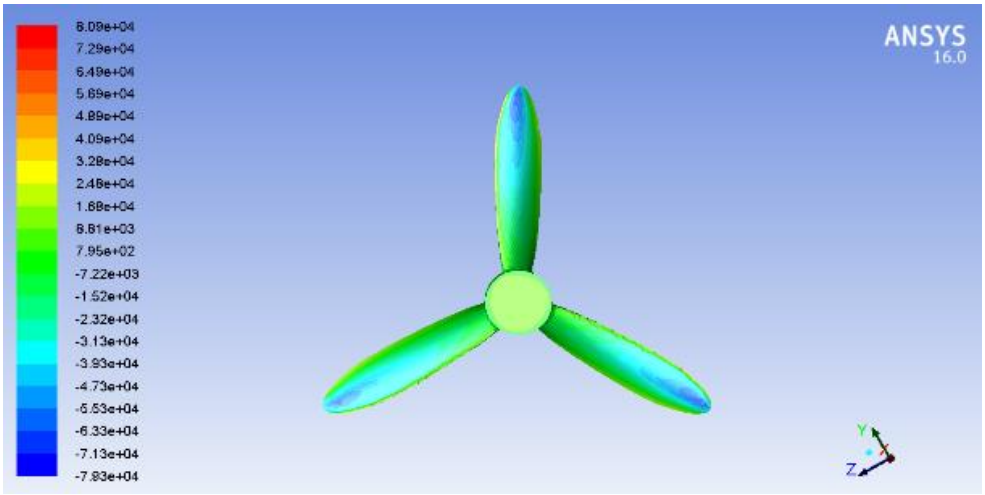

Figure 16. Propeller leaf back pressure cloud map.

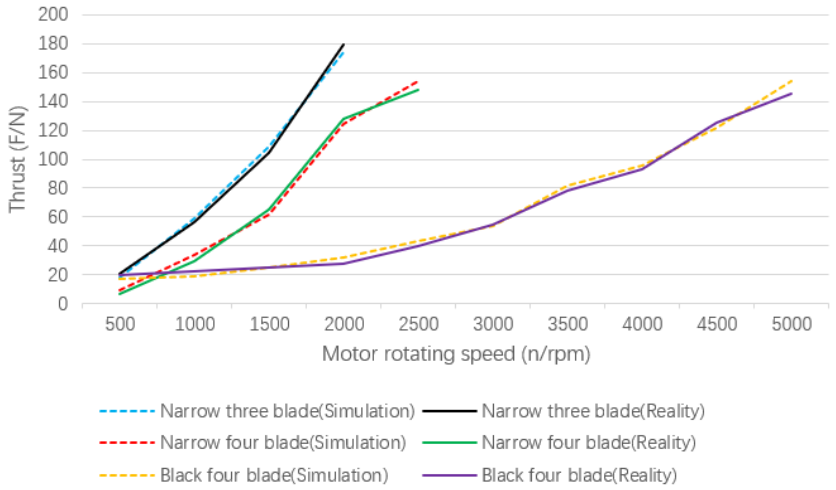

Figure 17. Relation curve between thrust and rotating speed.

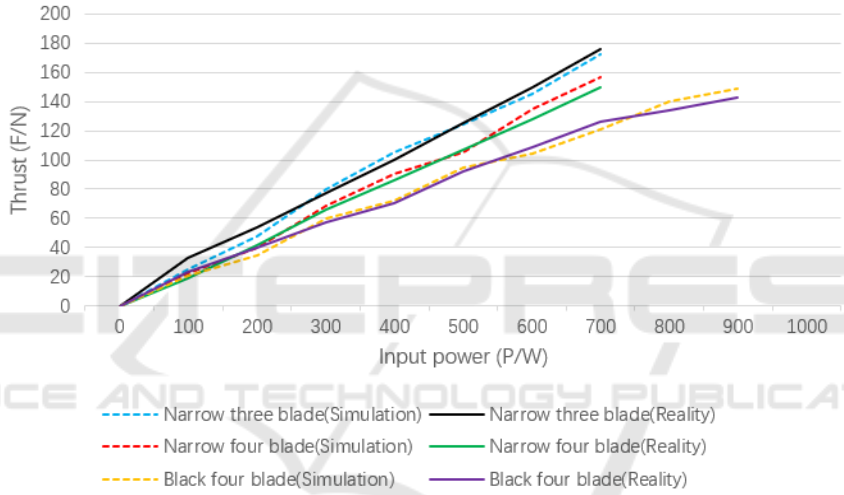

Figure 18. Relation curve between thrust and input power.

In the formula, p is static pressure. τij is the stress tensor. gi is the gravity volume force in the i direction. Fi is the external volume force in the i direction, Fi contains other model related source terms. ui and uj are the mean value of the velocity component in the xi and xj directions. ρ is the fluid density. μ is the fluid viscosity coefficient. Gk is the turbulent energy caused by the average velocity gradient. Gb is the turbulent energy caused by buoyancy. YM is influence of turbulent pulsation expansion on total dissipation rate. μt is the turbulent viscosity coefficient (X. F. Xue, T. H. Yan, B. He, 2016). The optimized propeller as shown in Fig.11 and Fig.12, and the mesh division and simulation results. As shown in Fig.13 to Fig.16.

In this paper, the numerical simulation calculation (N. Yilmaz, M. Atlar, M. Khorasanchi., 2019; N. Abbas, N. Kornev, I. Shevchuk, P. Anschau, 2015; D. Owen, Y. K. Demirel, E. Oguz, T. Tezdogan, A. Incecik, 2018; A. Dubois, Z. Q. Leong, H. D. Nguyen, J. R. Binns, 2019) uses speed inlet and pressure outlet, which is the same as the reference (Z. Q. Yao, H. Gao, C. L. Yang, 2008; W. G. He, 2014; X. S. Xie, Z. F. Jiang, L. Y. Qiu, 2015; J. M. Wu, Y. F. Lai, J. W. Li, 2016; F. D. Gao, C. Y. Pan, 2011). The setting conditions are speed inlet and free flow outlet in reference (H. P. Pei, R. Liu, 2018). Other setting conditions are similar. From the simulation results, the propeller accelerates the rear fluid. The water flows spirally through the propeller, and the diameter of the rear flow field is smaller than the diameter of the propeller. The fluid is dense and smooth. The blade leaf of the propeller is positive pressure, and the blade back leaf of the propeller is negative pressure. The pressure difference is large, indicating that the rotation of the

propeller produces a large thrust. The actual application results are basically consistent with the numerical simulation results, and the comparison results are shown in Fig.17 and Fig.18. In summary, the propeller has good hydrodynamic performance and meets the needs.

5 CONCLUSIONS

According to the parameters of the reference (R. S. Duelley, 2011), the propeller has not reached the ideal efficiency value after the actual measurement. In recent years, the research has not solved the efficiency problem well. In this paper, the design parameters are optimized based on the reference (R. S. Duelley, 2011). The propeller produces a large thrust while maintaining a high efficiency state. Parametric modeling of propellers based on OpenProp and SolidWorks, from theoretical analysis, parameter research to data import and complete three-dimensional modeling, saving a lot of time spend on data calculation, making propeller design and processing more convenient and faster. This test verifies the reliability of this design method by testing the actual application effect of the propeller and comparing it with the theoretical design. The test proves that the parametric modeling method by using OpenProp are reliable. The results of the thrust theoretical analysis are not much different from those of the actual application.

This experiment tests the actual hydrodynamic performance of the four propellers and draws the following conclusions. Under the premise that other parameters are consistent, the efficiency of the three-bladed propeller is higher than the four-bladed propeller. The efficiency of the narrow blade propeller is higher than the wide blade propeller. The efficiency of the small diameter propeller at high rotating speed is greater than that at low rotating speed. The efficiency of the large diameter propeller at low rotating speed is greater than that at high rotating speed. The change in back rake angle has little effect on the hydrodynamic performance of the propeller. For MAU type propeller tested in this paper, the efficiency of correct installation and reverse installation is very different. The correct installation efficiency is much higher than the reverse installation efficiency. However, the efficiency of airfoil propeller correct or reverse installation is not much different. And the hydrodynamic performance in the reverse installation is better than the MAU type propeller. That is, the map propeller is suitable for single way propulsion and the airfoil propeller is suitable for double way propulsion.

ACKNOWLEDGEMENTS

This work was financially supported by the National Key Research and Development Program of China (Grant No. 2016YFC0301404) and the National Natural Science Foundation of China (Grant No. 51379198).

REFERENCES

A. Bhattacharyya, V. Krasilnikov, S. Steen. A CFD-based scaling approach for ducted propellers. *Ocean Engineering*, 2016, 123, 116-130.

A. Dubois, Z. Q. Leong, H. D. Nguyen, J. R. Binns. Uncertainty estimation of a CFD-methodology for the performance analysis of a collective and cyclic pitch propeller. *Applied Ocean Research*, 2019, 85, 73-87.

B. An, H. H. Zhu, S. D. Fan. Three-dimensional modeling and performance analysis of an AU propeller. *China Ship Repair*, 2017, 30(3), 48-52.

C. Y. Liu, K. Luo, Q. Guo. Performance prediction of contra-rotating propellers for undersea vehicle. *Journal of Unmanned Undersea System*, 2017, 25(5), 437-442.

D. Owen, Y. K. Demirel, E. Oguz, T. Tezdogan, A. Incecik. Investigating the effect of biofouling on propeller characteristics using CFD. *Ocean Engineering*, 2018, 159, 505-516.

F. D. Gao, C. Y. Pan. Parameterized design and analysis of the complicated curved-surface propeller in solid modeling. *Mechanical Science and Technology for Aerospace Engineering*, 2011, 30(1), 1-5.

H. P. Pei, R. Liu. Three-dimensional modeling and hydrodynamic performance analysis of different pitch angle propeller. *Journal of Hangzhou Dianzi University (Natural Sciences)*, 2018, 38(2), 78-83.

J. M. Wu, E. W. Zhang, L. Zhong. Thrust characteristics of ducted propeller under the influence of cavitation. *Journal of South China University of Technology (Natural Science Edition)*, 2018, 46(1), 41-49.

J. M. Wu, L. Zhong, E. W. Zhang. Simulation of hydrodynamics of underwater robot in reverse propeller and negative speed. *Ship Engineering*, 2017, 39(S1), 225-229,292.

J. M. Wu, Y. F. Lai, J. W. Li. Distribution characteristics of thrust, advanced and induced velocity on ducted propeller disk. *Ship Engineering*, 2016, 38(12), 23-26, 36.

L. Huang, L. Chen. Propeller modeling method and open water performance study. *Ship Electronic Engineering*, 2014, 34(8), 78-80.

M. M. Helal, T. M. Ahmed, A. A. Banawan, M. A. Kotb. Numerical prediction of sheet cavitation on marine

propellers using CFD simulation with transition-sensitive turbulence model. *Alexandria Engineering Journa*l, 2018, 57, 3805-3815.

N. Abbas, N. Kornev, I. Shevchuk, P. Anschau. CFD prediction of unsteady forces on marine propellers caused by the wake nonuniformity and nonstationarity. *Ocean Engineering*, 2015, 104, 659-672.

N. Yilmaz, M. Atlar, M. Khorasanchi. An improved Mesh Adaption and Refinement approach to Cavitation Simulation (MARCS) of propellers. *Ocean Engineering*, 2019, 171, 139-150.

R. Muscari, G. Dubbioso, M. Viviani, A. D. Mascio. Analysis of the asymmetric behavior of propeller–rudder system of twin screw ships by CFD. *Ocean Engineering*, 2017, 143, 269-281.

R. S. Duelley. Autonomous underwater vehicle propulsion design. Master Thesis, Virginia Polytechnic Institute and State University, Blacksburg, 2011, pp.78.

S. Sezen, A. Dogrul, C. Delen, S. Bal. Investigation of self-propulsion of DARPA Suboff by RANS method. *Ocean Engineering*, 2018, 150, 258-271.

T. Zhang, C. J. Yang, B. W. Song. CFD simulation of the unsteady performance of contra-rotating propellers. *Journal of Ship Mechanics*, 2011, 15(6), 605-615.

W. G. He. Simulation calculation and analysis of vessel propeller's open water performance. *Ship Engineering*, 2014, 36(S1), 48-51.

W. H. Lam, D. J. Robinso, G. A. Hamill, H. T. Johnston. An effective method for comparing the turbulence intensity from LDA measurements and CFD predictions within a ship propeller jet. *Ocean Engineering*, 2012, 52, 105-124.

X. F. Xue, T. H. Yan, B. He. Modeling and hydrodynamic performance analysis of MAU propeller. *Ship Engineering*, 2016, 38(1), 38-42.

X. M. Wang, S. Feng. Simulation and analysis of hydrodynamic performance of propeller of small ROV. *Ship Engineering*, 2018, 40(S1), 321-324,345.

X. S. Xie, Z. F. Jiang, L. Y. Qiu. Study on propeller unsteady performance in viscous non-uniform wake. *Ship Engineering*, 2015, 37(6), 37-40, 62.

Y. F. Qin, X. J. Sun, X. H. Lin. Propulsive efficiency of low rotation propeller for underwater glider. *Journal of PLA University of Science and Technology (Natural Science Edition)*, 2017, 18(1), 61-67.

Y. W. Ding, J. M. Wu, Z. Q. Ma. Analysis of thrust characteristics of ducted propeller based on lattice boltzmann method. *Ship Engineering*, 2018, 40(S1), 104-109.

Z. Q. Yao, H. Gao, C. L. Yang. 3D modeling and numerical analysis for hydrodynamic force of propeller. *Ship Engineering*, 2008, 30(6), 23-26.